JB
Journals.ASM.org

Streptococcus pneumoniae Folate Biosynthesis Responds to Environmental CO_2 Levels

Peter Burghout,[a] Aldert Zomer,[a] Christa E. van der Gaast-de Jongh,[a] Eva M. Janssen-Megens,[b] Kees-Jan Françoijs,[b] Hendrik G. Stunnenberg,[b] Peter W. M. Hermans[a]

Laboratory of Pediatric Infectious Diseases, Radboud University Medical Center, Nijmegen, The Netherlands[a]; Department of Molecular Biology, Radboud University, Nijmegen Center for Molecular Life Sciences, Nijmegen, The Netherlands[b]

Although carbon dioxide (CO_2) is known to be essential for *Streptococcus pneumoniae* growth, it is poorly understood how this respiratory tract pathogen adapts to the large changes in environmental CO_2 levels it encounters during transmission, host colonization, and disease. To identify the molecular mechanisms that facilitate pneumococcal growth under CO_2-poor conditions, we generated a random *S. pneumoniae* R6 *mariner* transposon mutant library representing mutations in 1,538 different genes and exposed it to CO_2-poor ambient air. With Tn-seq, we found mutations in two genes that were involved in *S. pneumoniae* adaptation to changes in CO_2 availability. The gene *pca*, encoding pneumococcal carbonic anhydrase (PCA), was absolutely essential for *S. pneumoniae* growth under CO_2-poor conditions. PCA catalyzes the reversible hydration of endogenous CO_2 to bicarbonate (HCO_3^-) and was previously demonstrated to facilitate HCO_3^--dependent fatty acid biosynthesis. The gene *folC* that encodes the dihydrofolate/folylpolyglutamate synthase was required at the initial phase of bacterial growth under CO_2-poor culture conditions. FolC compensated for the growth-phase-dependent decrease in *S. pneumoniae* intracellular long-chain ($n > 3$) polyglutamyl folate levels, which was most pronounced under CO_2-poor growth conditions. In conclusion, *S. pneumoniae* adaptation to changes in CO_2 availability involves the retention of endogenous CO_2 and the preservation of intracellular long-chain polyglutamyl folate pools.

The human-restricted respiratory tract pathogen *Streptococcus pneumoniae* is a leading cause of otitis media, pneumonia, bacteremia, and meningitis. This Gram-positive bacterium is also a commensal of the human upper respiratory tract, with nasopharyngeal carriage rates of around 10% in adults and over 40% in children (1). The high rate of *S. pneumoniae* nasopharyngeal colonization and its ability to cause disease underline the fact that this pathogen is well adapted to the human host. Research on components that physically contribute to host-pathogen interaction, e.g., capsular polysaccharides, adhesins, and toxins, has provided valuable insights into the process of pneumococcal pathogenesis (2). In contrast, the influence of environmental factors on pneumococcal growth has remained largely unexplored.

The exposure of *S. pneumoniae* to ambient air can have a pronounced influence on bacterial growth. There is increasing evidence that this behavior relates to the reduced availability of environmental CO_2, which is as low as 0.038% in ambient air. For instance, about 8% of all clinical *S. pneumoniae* isolates need a CO_2-enriched environment for growth (3). Moreover, under CO_2-depleted laboratory conditions, the growth of all pneumococcal strains is impaired (4). The intrinsic dependence of (micro)-organisms on CO_2 is often related to an anabolic need for CO_2 or bicarbonate (HCO_3^-) during, for instance, biosynthesis of nucleic acids, amino acids, and fatty acids (5, 6, 7). Microbial pathogens can sequester CO_2 from CO_2-rich host tissues, but under CO_2-poor conditions, such as the ambient air outside the host, retention of endogenously produced CO_2 is required to maintain adequate levels of intracellular CO_2. We have recently shown that pneumococcal carbonic anhydrase (PCA), which catalyzes the reversible hydration of CO_2 to HCO_3^-, is essential for the cellular retention of CO_2 (8). *S. pneumoniae* Δ*pca* strains were impaired for growth in ambient air unless cultures were supplemented with CO_2, HCO_3^-, or unsaturated fatty acid. Interestingly, the growth characteristics of naturally occurring CO_2-dependent *S. pneumoniae* isolates, so-called capnophils, could not be explained by the absence of the *pca* gene (8). Hence, there is still much to learn about the CO_2-dependent molecular mechanisms that are essential for pneumococcal growth.

Mutant library screening has proven to be a powerful approach to link microbial genes to cell function (9, 10). In this strategy, mutant libraries are challenged by an *in vivo* or *in vitro* stress condition to counterselect for mutants in which a conditionally essential gene has been disrupted. Readout of mutant-specific probes will reveal which mutants fail to grow during challenge and, consequently, which genes are conditionally essential. Despite its limitations, e.g., cross-complementation of some mutants by diffusible (gene) products, a mutant library screen remains the fastest approach to assess gene essentiality in a genomewide manner. Recently, next-generation sequencing (NGS) has been applied to track large microbial transposon mutant libraries (11, 12, 13). In this so-called Tn-seq technology, mutant-specific DNA probes are generated by PCR amplification of the genomic DNA around the transposon insertion site. Since the site of mutagenesis is revealed exactly, this technology has further improved the throughput and accuracy of mutant library screens.

In this study, we used the Tn-seq technology to identify *S. pneumoniae* genes that are required to cope with the changes in

Received 1 October 2012 Accepted 22 January 2013
Published ahead of print 25 January 2013
Address correspondence to Peter W. M. Hermans, p.hermans@cukz.umcn.nl, or Peter Burghout, p.j.burghout@gmail.com.

doi:10.1128/JB.01942-12

TABLE 1 Bacterial strains and plasmids in this study

Strain	Relevant characteristics[a]	Reference or source
S. pneumoniae strains		
R6	Wild-type strain, unencapsulated	19
LKIPB01	R6 Δ*pca* Sp^r	8
LKIPB02	R6 Δ*folC* Sp^r	This study
LKIPB03	R6 Δ*ogt* Sp^r	This study
LKIPB04	R6 CEP^- Km^r	This study
LKIPB05	R6 CEP^{folC} Km^r	This study
LKIPB06	R6 Δ*folC* CEP^- Sp^r Km^r	This study
LKIPB07	R6 Δ*folC* CEP^{folC} Sp^r Km^r	This study
E. coli DH5α	Cloning strain	40
L. casei ATCC 7469	Folic acid-dependent strain	ATCC

[a] Sp^r, spectinomycin resistant; Km^r, kanamycin resistant.

environmental CO_2 levels this respiratory tract pathogen will encounter inside and outside the host during transmission, host colonization, and disease.

MATERIALS AND METHODS

Bacterial strains and growth conditions. The bacterial strains used in this study are listed in Table 1. *S. pneumoniae w*as grown routinely in brain heart infusion (BHI) broth (Difco) with 400 U ml^{-1} bovine liver catalase (Sigma) or on blood agar (BA) plates composed of Colombia agar (Oxoid) supplemented with 5% sheep blood (Biotrading) at 37°C and 5% CO_2. To compare growth under CO_2-poor and CO_2-rich conditions, bacteria were grown in medium exposed overnight to ambient air (~0.038% CO_2) or to ambient air enriched with 5% CO_2, respectively. For monocultures, 15% glycerol stocks of *S. pneumoniae* mid-log-phase cultures in CO_2-rich medium were pelleted by centrifugation, washed in CO_2-poor phosphate-buffered saline (PBS) or BHI broth, and diluted 100-fold in prewarmed CO_2-poor or CO_2-rich BHI broth. For competition experiments, a 1:1 mixture of the *S. pneumoniae* wild type and the mutant strain was inoculated at 10^6 CFU ml^{-1} and grown for approximately 6 h. Viable bacterial counts were derived by enumerating CFU after plating 10-fold serial dilutions in PBS on BA plates and/or BA plates supplemented with spectinomycin. For samples in which no viable bacteria were recovered, the lower limit of detection (20 CFU ml^{-1}) was substituted as the numerator. *Escherichia coli* was grown on Luria Bertani (LB) agar plates or in LB broth in a 200-rpm shaking incubator at 37°C. Genetic transformation of *S. pneumoniae* and *E. coli* was performed as described previously (14, 15). *Lactobacillus casei* (also known as *Lactococcus rhamnosus*) was grown in folic acid casei (FAC) medium supplemented with 0.3 μg $liter^{-1}$ folate and 250 mg $liter^{-1}$ sodium ascorbate at 37°C with 5% CO_2, and freezer stocks were prepared with 40% glycerol. When indicated, antibiotics were used at the following concentrations: spectinomycin, 150 μg ml^{-1} for *S. pneumoniae*, and kanamycin, 50 μg ml^{-1} for *E. coli* and 500 μg ml^{-1} for *S. pneumoniae*. The maltose-inducible promoter on the chromosomal expression platform (CEP) ectopic expression system was activated with 0.4% maltose. The aqueous stock solution for the metabolic complementation assays was composed of 10 mg ml^{-1} adenosine, 100 mg ml^{-1} glycine, 25 mg ml^{-1} methionine, 2 mg ml^{-1} pantothenate, 100 mg ml^{-1} serine, 1 M sodium bicarbonate, and 20 mg ml^{-1} thymidine.

DNA extraction, amplification, and quantification. Genomic DNA was isolated from *S. pneumoniae* broth cultures with the Qiagen Genomic-tip system (Qiagen). Plasmids were isolated from *E. coli* broth cultures with the QIAprep minikit (Qiagen). In PCRs needed for the construction of plasmids and the *S. pneumoniae* mutant strains, the proofreading *Pwo* DNA polymerase (Roche) was used. For Tn-seq DNA probe synthesis, the Phusion DNA polymerase (Bioke) and high-fidelity (HF) buffer were used. For other PCR-based approaches, AmpliTaq DNA polymerase (Applied Biosystems) was applied. The primers (Biolegio) that were used in this study are listed in Table 2. All Tn-seq primers were PAGE purified. Standard measurements of DNA concentrations were performed with a Nanodrop (Thermo Fisher Scientific), but for Tn-seq probes, a Qubit (Invitrogen) was used.

TABLE 2 Primers used in this study

Purpose and primer	Nucleotide sequence (5′–3′)[a]
Deletion mutant construction	
CvdGspr0178_L1	TGGAGGAGTGATACAGTCTG
CvdGspr0178_L2	CCACTAGTTCTAGAGCGGCAACCAATCCGACT ATGGAGC
CvdGspr0178_R1	ATTTGGTCCGATGGGTCTC
CvdGspr0178_R2	GCGTCAATTCGAGGGGTATCGACTTGCTGTTC GTTACAGG
CvdGspr0178_C	ATAGGGTAAGACTGCTCAGG
CvdGspr1317_L1	AGTAGATGCCATCATGCAGG
CvdGspr1317_L2	CCACTAGTTCTAGAGCGGCAATTGGTGAGGAG TAGAGG
CvdGspr1317_R1	TGCTACGGTCAGATACAGAC
CvdGspr1317_R2	GCGTCAATTCGAGGGGTATCTTGGAGCATGAA GGAGTAG
CvdGspr1317_C	TGCTCCTGAACCCAAATTCC
Plasmid construction	
PBGSF20	P-ACAGGTTGGATGATAAGTCCCCGGTCT
M13fw	GTAAAACGACGGCCAGT
M13rev	CAGGAAACAGCTATGAC
PBfolCN	GTAGCCATGGGTATGTTTGAAGTAAAAGAATGG
PBfolCB2	CTTAAGATCTTCAATTTATCTGCTCACGGTC
Tn-seq	
PBGSF23	CAAGCAGAAGACGGCATACGAAGACCGGGGA CTTATCATCCAACCTGT
PBGSF29 ATCACG	TTCCCTACACGACGCTCTTCCGATCTATCACGNN
PBGSF30 ATCACG	P-CGTGATAGATCGGAAGAGCGTCGTGTAGGG AAAGAGT-P
PBGSF29 CGATGT	TTCCCTACACGACGCTCTTCCGATCTCGATGTNN
PBGSF30 CGATGT	P-ACATCGAGATCGGAAGAGCGTCGTGTAGGG AAAGAGT-P
PBGSF29 TTAGGC	TTCCCTACACGACGCTCTTCCGATCTTTAGGCNN
PBGSF30 TTAGGC	P-GCCTAAAGATCGGAAGAGCGTCGTGTAGGG AAAGAGT-P
PBGSF29 TGACCA	TTCCCTACACGACGCTCTTCCGATCTTGACCANN
PBGSF30 TGACCA	P-TGGTCAAGATCGGAAGAGCGTCGTGTAGGG AAAGAGT-P
PBGSF31	AATGATACGGCGACCACCGAGATCTACACTCT TTCCCTACACGACGCTCTTCCGATCT

[a] P, phosphorylated.

Plasmid construction. All plasmids used in this study are listed in Table 3 and were generated and maintained in *E. coli* cells. To make the genomic array footprinting (GAF) pR412T7 plasmid (9) suitable for Tn-seq, the pR412T7 *mariner* transposon was PCR amplified with a single 5′-phosphorylated PBGSF20 primer. The PCR cycling conditions were as follows: 93°C for 4 min; 30 cycles of 93°C for 30s, 50°C for 30s, and 68°C for 2 min; and 68°C for 5 min. The PCR introduced an MmeI endonuclease site in the inverted repeats of the *mariner* transposon. This *mariner* transposon PCR product was cloned into the pCR2.1 vector of the TA cloning kit (Invitrogen) to obtain pGSF8. Correct integration of the MmeI sites was confirmed by Sanger sequencing with M13fw and M13rev primers.

TABLE 3 Plasmids used in this study

Plasmid	Relevant characteristics[a]	Reference or source
pR412	Donor for Sp^r cassette, Amp^r Sp^r	41
pR412T7	Donor for *mariner* transposon, Amp^r Sp^r	9
pGSF8	Donor for *mariner* transposon, Amp^r Sp^r Km^r	This study
pCO2.1	pCR2.1 with *S. pneumoniae* R6 spr0178 (*folC*) gene	This study

[a] Sp^r, spectinomycin resistant; Amp^r, ampicillin resistant; Km^r, kanamycin resistant.

To enable ectopic expression of FolC in the *S. pneumoniae* LKIPB02 (Δ*folC*) strain, the spr0178 gene was PCR amplified with the PBfolCN and PBfolCB2 primer pair and cloned into pCR2.1 of the TA cloning kit (Invitrogen) to obtain pCO2.1.

***S. pneumoniae* mutant library construction and challenge conditions.** *S. pneumoniae* R6 transposon mutant libraries were generated essentially as described previously (14). Briefly, 0.5 μg of *S. pneumoniae* genomic DNA was incubated for 4 h with purified HimarC9 transposase and 0.5 μg of pGSF8 plasmid. After repair of the resulting transposition products with T4 DNA polymerase and *E. coli* DNA ligase, 100 ng mutagenized DNA was used for transformation of 1 ml precompetent *S. pneumoniae* cells. For mutant library construction, the required number of colonies was scraped from the plates, pooled, and grown to mid-log phase in CO_2-rich BHI, and aliquots were stored with 15% glycerol at −80°C. *S. pneumoniae* R6 transposon mutant libraries were challenged for a total of ~24 generations in either CO_2-poor (3 replicates) or CO_2-rich (4 replicates) BHI. To achieve this, mid-log cultures of the mutant library were diluted 100-fold, grown to mid-log phase, and stored in 15% glycerol at −80°C. This procedure was repeated for a total of 3 times. After the 3rd round of growth, chromosomal DNA was isolated for Tn-seq analysis. Generation times were confirmed by viable bacterial counts.

Tn-seq analysis of *S. pneumoniae mariner* transposon mutant libraries. The Tn-seq technology was performed essentially as described previously (13), with minor modifications. Briefly, a 200-μl solution with 2 μg *S. pneumoniae* mutant library genomic DNA in NEBuffer 4 (New England BioLabs) with 5 μM *S*-adenosylmethionine was digested with 10 U MmeI (New England BioLabs) for 4 h at 37°C and dephosphorylated with 1 U calf intestine alkaline phosphatase (Invitrogen) for 30 min at 50°C. Next, the reaction mixture was successively extracted with 200 μl phenol-chloroform-isoamyl alcohol (25:24:1) and with 200 μl chloroform-isoamyl alcohol (24:1) and was ethanol precipitated, and the dried DNA pellet was dissolved in 20 μl H_2O. Tn-seq adapters with a 6-bp barcode were prepared by combining 5 nmol of two matching barcoded PBGSF29 and PBGSF30 oligonucleotides (Table 2) in 1× Tris-EDTA and 50 mM NaCl in a total volume of 50 μl and performing a 10-min denaturation step at 95°C and an annealing step in which the reaction mixture was slowly cooled to room temperature. A 20-μl solution with 200 pmol annealed adapter was phosphorylated with T4 polynucleotide kinase (3′ phosphatase minus) (New England BioLabs) in T4 DNA ligase buffer (New England BioLabs) for 5 min at 37°C and heat inactivated for 10 min at 70°C. Ligation of 100 ng dephosphorylated MmeI restriction fragments with 2 pmol phosphorylated adapter was performed in the presence of T4 DNA ligase buffer with 2 U T4 DNA ligase (New England BioLabs) in a total volume of 20 μl for 1 h at 16°C. Immediately after the ligation, Tn-seq DNA probes were generated by PCR with 2.5 μl ligation reaction product as the template, 20 pmol PBGSF23 and PBGSF31 primers, HF buffer, 0.2 mM deoxynucleoside triphosphate mix, and 1 U Phusion DNA polymerase in a total volume of 50 μl. The PCR cycling conditions were as follows: 72°C for 1 min and 98°C for 30 s; 25 cycles of 98°C for 30 s, 57°C for 30 s, and 72°C for 10 s; and 72°C for 5 min. The resulting PCR products of ~130 bp were purified from the PCR with the Minelute reaction cleanup kit (Qiagen). After pooling of samples with up to four different 6-bp barcodes, typically 9 fmol Tn-seq DNA probes were loaded on a Genome Analyzer II (Illumina) for sequence analysis with the manufacturer's protocols, using the genomic DNA sequencing primer (Illumina) and 36 sequencing cycles.

Data analysis. Tn-seq data analysis was performed as described previously (16). Briefly, FASTQ files of the Tn-seq results were imported to the web-based interface ESSENTIALS (bamics2.cmbi.ru.nl/websoftware/essentials) and extracted with default settings. Count data (i.e., pseudoreads) were generated per unique sequence read or per gene and corrected by locally weighted scatterplot smoothing (LOESS) for the bias in Tn-seq data caused by the increase in available DNA close to the origin of replication (ORI). Normalization factors were calculated using trimmed mean of *M* values (TMM). Pseudoreads in the control and target samples were tested for significant differences ($P \leq 0.001$) by a quantile-adjusted conditional maximum likelihood (qCML) method assuming moderated tagwise dispersion of replicates. The prior.*n* value to determine the amount of smoothing of tagwise dispersions was set at 5. *P* value adjustment (adjusted $P \leq 0.05$) was based on the Benjamini-Hochberg procedure. Gene essentiality was determined by comparing the expected number of pseudoreads per gene (based on the number of transposon insertion sites per gene, the mutant library size, and the sequencing depth) and the measured number of pseudoreads per gene. Significantly underrepresented genes were considered essential and omitted from the data analysis. All data can be found on the ESSENTIALS website http://bamics2.cmbi.ru.nl/websoftware/essentials/links.html.

Construction of *S. pneumoniae* mutant strains. Directed-deletion mutants of *S. pneumoniae* were generated by allelic exchange of the target gene with an antibiotic resistance marker as described previously (14). For genetic complementation of the LKIPB02 (Δ*folC*) strain, the *folC* gene was excised from the pCO2.1 plasmid by NcoI/BglII digestion and ligated into the NcoI/BamHI-digested pCEP plasmid (17). The pCEP-*folC* ligation mixture was immediately transformed into *S. pneumoniae*. Because pCEP is unable to replicate in *S. pneumoniae*, CEP^{folC} strains (i.e., LKIPB05 and LKIPB07) have acquired an ectopic copy of the *folC* gene behind a maltose-inducible promoter on the *S. pneumoniae* chromosome. As a control, *S. pneumoniae* was transformed with the empty pCEP plasmid to obtain CEP^- strains (LKIPB04 and LKIPB06).

Microbiological folate assay. Intracellular total and short-chain ($n \leq 3$) polyglutamyl folate were quantified using an *L. casei* microbiological assay (18). Briefly, *S. pneumoniae* mid-log-phase cultures that were washed in CO_2-poor BHI were diluted 10- or 100-fold in CO_2-poor and CO_2-rich BHI medium and bacterial cells were recovered after 1 or 6 h of incubation, respectively, at 37°C. Next, cells were washed 3 times in 2× FAC medium (Difco) and viable bacterial counts were determined after the last wash step. Then, cell suspensions in 2× FAC medium were diluted 5-fold in lysis buffer (0.1 M NaAc buffer, pH 4.8, 1% ascorbic acid) and incubated at 100°C for 5 min. To determine total folate levels, samples were pretreated for 4 h at 37°C with 2.5% (vol/vol) of the soluble fraction of a human plasma solution (1 g human plasma [Sigma] in 5 ml 0.1 M 2-mercaptoethanol and 0.5% sodium ascorbate) to deconjugate polyglutamyl folate. A 1% yeast extract solution (Difco) was used as a positive control for the deconjugation reaction. Prior to the microbiological assay, *L. casei* cells from freezer stocks were washed 3 times in folate-free 2× FAC medium. The microbiological folate assay was performed in 96-well flat-bottom plates containing 95 μl 2× FAC medium with a 100-fold dilution of washed *L. casei* cells, 95 μl 2× folate assay buffer (0.1 M potassium phosphate buffer, pH 6.3, containing 1% ascorbic acid), and 10-μl amounts of the samples or standards in lysis buffer. The concentrations of the standards in the assay were 0, 10, 20, 40, 80, 120, 160, and 200 pg ml^{-1} folic acid. Readout of the plate occurred at an optical density of 620 nm (OD_{620}). All folate assays were performed three times in triplicate. Intracellular folate concentrations were related to bacterial viable counts.

Statistics. A competitive index (CI) score, expressing the relative growth defect of the *S. pneumoniae* mutant compared to the growth of the wild-type strain, was calculated by dividing the ratio of the viable bacterial counts of mutant to wild-type bacteria in CO_2-poor ambient air by the ratio of the viable bacterial counts of mutant to wild-type bacteria under CO_2-rich conditions. A one-sample *t* test on log-transformed CI scores (with an arbitrary mean of 0 and a *P* value of < 0.05) was used to calculate statistical significance. In noncompetitive experiments, unpaired *t* tests were used to evaluate the significance of differences in bacterial viable counts and intracellular folate levels. Statistical analyses were performed using GraphPad Prism, version 4.0 (GraphPad Software, Inc., La Jolla, CA).

RESULTS

Tn-seq analysis of an *S. pneumoniae* mutant library challenged by CO_2-poor conditions. In order to identify genes essential for pneumococcal growth in CO_2-poor conditions, we constructed

TABLE 4 Genes essential for *S. pneumoniae* R6 growth under CO_2-poor conditions

Locus	Gene	Description	Avg no. of pseudoreads[a] in indicated expt		Log^2 ratio of pseudoreads	Adj *P* value[b]
			Challenge	Control		
spr0026	*pca*	Carbonic anhydrase	86	1,149	−3.74	1.3×10^{-6}
spr0178	*folC*	DHFS/FPGS	168	2,469	−3.88	3.7×10^{-7}
spr1317	*ogt*	6-*O*-Methylguanine-DNA methyltransferase	11	100	−3.17	9.5×10^{-4}

[a] Average of the normalized sequence reads.
[b] Benjamini and Hochberg adjusted *P* value.

an *S. pneumoniae* R6 mutant library composed of 40,000 independent *mariner* transposon mutants under 5% CO_2-enriched culture conditions. Subsequently, this mutant library was challenged by growth under ambient air (~0.04% CO_2, i.e., challenge) and CO_2-rich (5% CO_2, i.e., control) culture conditions for 24 generations. Under the control conditions, Tn-seq analysis revealed 14,023 unique transposon mutations with at least 20 sequence reads, representing a total of 1,538 different genes. Under the challenge conditions, there were significant decreases in the numbers of pseudoreads, i.e., normalized Tn-seq readout data, for the spr0026 (*pca*), spr0178 (*folC*), and spr1317 (*ogt*) genes (Table 4). Similarly, we found a considerable conditional change in the number of pseudoreads for each individual transposon mutation in these target genes (Table 5). Of note, the number of pseudoreads for each individual transposon mutation in the *ogt* gene was very close to the detection limit.

Growth of the *S. pneumoniae* Δ*pca* and Δ*folC* strains is CO_2 dependent. To examine whether the Tn-seq target genes were indeed required for *S. pneumoniae* growth under CO_2-poor conditions, the LKIPB01, LKIPB02, and LKIPB03 strains were generated by allelic replacement of the *pca*, *folC*, and *ogt* gene, respectively, with a spectinomycin resistance cassette. To mimic the experimental setup of the mutant library screen, the validation experiments with the LKIPB01, LKIPB02, and LKIPB03 strains were performed in a competition setup with the R6 strain. These experiments showed that after 6 h of growth under CO_2-poor conditions, the LKIPB01 strain was outcompeted by the R6 strain by about 1,000-fold (Fig. 1). The LKIPB02 strain was also outcompeted by the R6 strain, but the difference was only 3-fold. The growth behavior of the LKIPB03 strain proved to be similar to that of the R6 strain, which means that the *ogt* gene is not required for *S. pneumoniae* adaptation to CO_2-poor conditions.

Next, we explored whether the CO_2-dependent growth restriction of the LKIPB01 and LKIPB02 strains also occurred in monoculture. We observed different CO_2-dependent growth phenotypes for the LKIPB01 and LKIPB02 strains. The growth restriction of the LKIPB01 strain became more pronounced after several hours of incubation under CO_2-poor conditions, after which we observed a complete growth arrest followed by a rapid decrease in cell viability and culture optical density (Fig. 2A and B). The growth restriction of the LKIPB02 strain under CO_2-poor conditions was most pronounced at 2 h postinoculation. At this

TABLE 5 Transposon mutants with mutations in the *S. pneumoniae* R6 *pca*, *folC*, and *ogt* genes

Target gene (position) and transposon insertion site	Read strand[a]	Avg no. of pseudoreads[b] in indicated expt		Log^2 ratio of pseudoreads	Adj *P* value[c]
		Challenge	Control		
pca (27115 to 27681)					
27138	−	44	596	−3.74	0.09
27138	+	47	444	−3.23	0.46
27518	−	1	39	−4.78	0.14
27518	+	4	215	−5.66	1.6×10^{-3}
folC (185813 to 187069)					
186202	−	9	94	−3.28	0.54
186202	+	11	309	−4.86	0.10
186450	−	56	798	−3.84	0.18
186450	+	47	551	−3.53	0.10
186814	−	31	500	−4.02	0.06
186814	+	18	613	−5.13	1.7×10^{-3}
ogt (1305516 to 1306046)					
1305654	−	1	26	−4.17	0.79
1305654	+	1	19	−3.75	0.65
1305973	−	3	22	−2.60	1
1305973	+	6	15	−1.25	1

[a] Orientation of the sequence read on the *S. pneumoniae* R6 genome.
[b] Average of the normalized sequence reads.
[c] Benjamini and Hochberg adjusted *P* value.

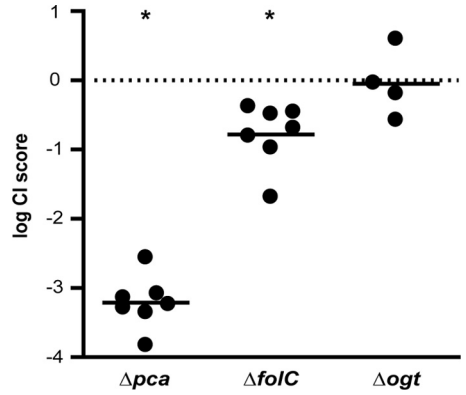

FIG 1 Competitive growth of the *S. pneumoniae* Δ*pca*, Δ*folC*, and Δ*ogt* strains. Mid-log-phase cultures of the LKIPB01 (Δ*pca*), LKIPB02 (Δ*folC*), and LKIPB03 (Δ*ogt*) strains were mixed 1:1 with the R6 strain under CO_2-poor versus CO_2-rich conditions, and the competitive index (CI) score was determined at approximately 6 h postinoculation. Symbols and horizontal lines mark individual and mean $\log_{10}$ CI scores, respectively, from cultures after approximately 6 h of growth. Asterisks mark $\log_{10}$ CI scores that are significantly different from zero ($P < 0.05$).

point, the bacterial viable counts and culture optical density under the CO_2-poor conditions were approximately 2-fold lower than the bacterial viable counts and culture optical density under the CO_2-rich conditions (Fig. 2A and B). At 4 h postinoculation, no further increases in the conditional differences between the bacterial viable counts and culture optical density were observed, suggesting that the conditional growth restriction of LKIPB02 occured only at the start of bacterial growth. At 6 h postinoculation, the culture optical density of the LKIPB02 strain under CO_2-poor conditions was still lower than the culture optical density under the CO_2-rich conditions. In contrast, the bacterial viable counts for the CO_2-poor and CO_2-rich culture conditions had become equal. This means that at this point, the culture under CO_2-rich conditions had already reached a different growth phase, while the culture under CO_2-poor conditions still experienced rapid exponential growth and a concomitant rise in bacterial viable counts.

To confirm that the CO_2-dependent growth phenotype of the LKIPB02 strain was a direct consequence of inactivation of the *folC* gene itself, the LKIPB02 strain was genetically complemented by ectopic expression of the *folC* gene from the maltose-inducible promoter of the chromosomal CEP platform (17). In a competition setup with the LKIPB05 (CEP^{folC}) strain, the LKIPB07 (Δ*folC* CEP^{folC}) strain was no longer attenuated for growth under CO_2-poor conditions (Fig. 3A). In contrast, the LKIPB06 (Δ*folC* CEP^{-}) strain was readily outcompeted by the LKIPB04 (CEP^{-}) strain. Also, in a monoculture, the LKIPB07 strain was rendered independent of CO_2 for growth (Fig. 3B). At the same time, the conditional growth characteristics of the LKIPB04 and LKIPB05 strain were identical (Fig. 3C). Of note, the addition of maltose was not required to restore the growth of the LKIPB07 strain (data not shown), which suggests that in our experimental setup, the maltose-inducible promoter was leaky. This suggests that the

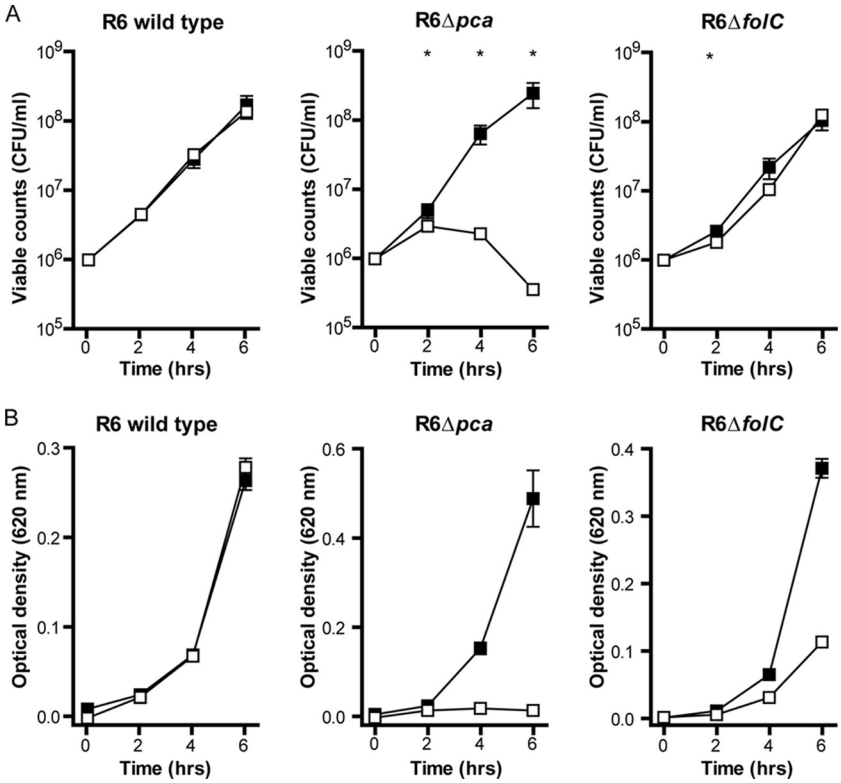

FIG 2 CO_2-dependent growth restriction of the *S. pneumoniae* Δ*pca* and Δ*folC* strains. The growth of the *S. pneumoniae* R6, LKIPB01 (R6Δ*pca*), and LKIPB02 (R6Δ*folC*) strains in CO_2-poor (open squares) or CO_2-rich (closed squares) BHI broth cultures was monitored by measuring the bacterial viable counts (A) and the optical density at 620 nm (B). Error bars represent standard deviations. (A) Asterisks mark time points at which the bacterial viable counts for the cultures under CO_2-poor or CO_2-rich conditions were significantly different ($P < 0.05$).

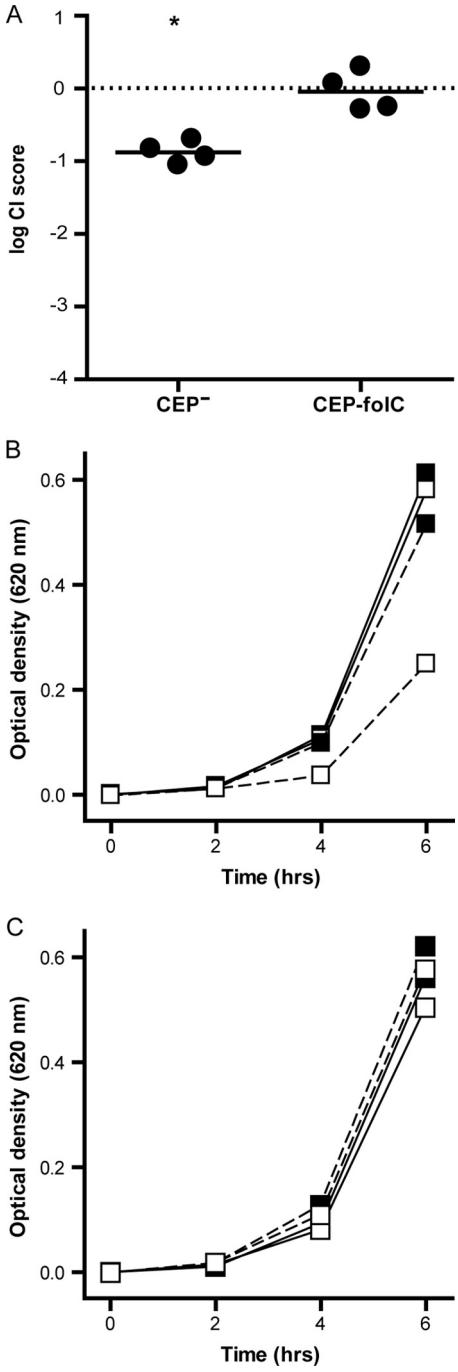

FIG 3 Genetic complementation of the *S. pneumoniae* R6 Δ*folC* strain. (A) Competitive growth of the LKIPB06 (Δ*folC* CEP$^-$) strain with the LKPBI04 (CEP$^-$) strain and of the LKIPB07 (Δ*folC* CEP^{folC}) strain with the LKIPB05 (CEP^{folC}) strain under CO_2-poor versus CO_2-rich conditions. Symbols and horizontal lines mark individual and mean $\log_{10}$ CI scores, respectively, from cultures after approximately 6 h of growth. Asterisks mark $\log_{10}$ CI scores that are significantly different from zero ($P < 0.05$). (B and C) Monocultures of the LKIPB06 strain (dashed lines) and the LKIPB07 strain (solid lines) (B) and of the LKIPB04 strain (dashed lines) and LKIPB05 strain (solid line) (C) were grown in BHI. Growth under CO_2-poor (open squares) and CO_2-rich (closed squares) conditions was monitored by measuring the optical density.

presence of FolC is important for *S. pneumoniae* adaptation to CO_2-poor growth conditions, whereas the FolC expression level is less relevant.

The *folC* gene is involved in *S. pneumoniae* long-chain polyglutamyl folate biosynthesis. The *S. pneumoniae pca* and *folC* genes encode pneumococcal carbonic anhydrase and the dihydrofolate/folylpolyglutamate synthase (DHFS/FPGS), respectively. PCA was previously shown by us to catalyze the reversible hydration of CO_2 to HCO_3^-, which is essential for the HCO_3^--dependent biosynthesis of unsaturated fatty acid under CO_2-poor conditions (8). The FolC DHFS/FPGS enzyme is annotated to catalyze the ATP-dependent glutamylation of dihydropteroate and/or polyglutamylation of tetrahydrofolate (19), which are essential for folate biosynthesis and the intracellular retention of folate, respectively. A microbiological folate assay was used to confirm that the LKIPB02 growth restriction in a CO_2-poor environment was related to a change in folate biosynthesis. We found that disruption of the *folC* gene resulted in a small but significant reduction in total intracellular folate levels at 1 h postinoculation (Fig. 4A). This phenomenon was observed under CO_2-rich conditions, as well as under CO_2-poor growth conditions, but the total intracellular folate level was the lowest under the CO_2-poor culture conditions. At 6 h postinoculation, we also observed a modest decrease in the total intracellular folate level upon removal of the *folC* gene and/or CO_2, but this was mostly not significant. Since FolC is predicted to have both dihydrofolate and folylpolyglutamate synthase activity, we also measured the composition of the different intracellular polyglutamyl folate pools. Based on the equal response of the microbiological folate assay for mono-, di-, and triglutamyl folate (20), there was no significant change in the intracellular short-chain ($n \leq 3$) polyglutamyl folate levels between the R6 and LKIPB02 strains (Fig. 4B). However, we did observe a small but significant change between the R6 and LKIPB02 short-chain polyglutamyl folate levels under CO_2-rich and CO_2-poor conditions at 6 and 1 h postinoculation, respectively. Finally, we measured intracellular long-chain ($n > 3$) polyglutamyl folate levels. At 1 h postinoculation under CO_2-rich conditions, the LKIPB02 intracellular long-chain polyglutamyl folate level was already 3-fold lower than in the R6 strain. Under the CO_2-poor growth conditions, this difference had become 10-fold, which was the direct consequence of a further decrease in the LKIPB02 intracellular long-chain polyglutamyl folate level. At 6 h postinoculation, the long-chain polyglutamyl folate levels were low for both strains under all conditions. However, there was a small but significant increase in LKIPB02 long-chain polyglutamyl folate levels under CO_2-rich conditions. Altogether, these findings suggest that FolC is implicated in long-chain polyglutamate folate biosynthesis in a growth-phase-dependent manner.

Folate-dependent metabolites do not rescue the growth defect of the *S. pneumoniae* Δ*folC* strain under CO_2-poor conditions. Folate is an important cofactor for various metabolic pathways. To link the growth defect of the LKIPB02 strain under CO_2-poor conditions to a specific metabolic pathway, we complemented LKIPB02 cultures under CO_2-poor and CO_2-rich conditions with sodium bicarbonate ($NaHCO_3^-$), folic acid, and the folate-dependent metabolites adenosine, glycine, methionine, pantothenate, serine, and thymidine. As expected, $NaHCO_3^-$ fully restored the growth of the LKIPB02 strain under CO_2-poor conditions to wild-type levels (Fig. 5). In contrast, supplementation with folic acid and folate-dependent

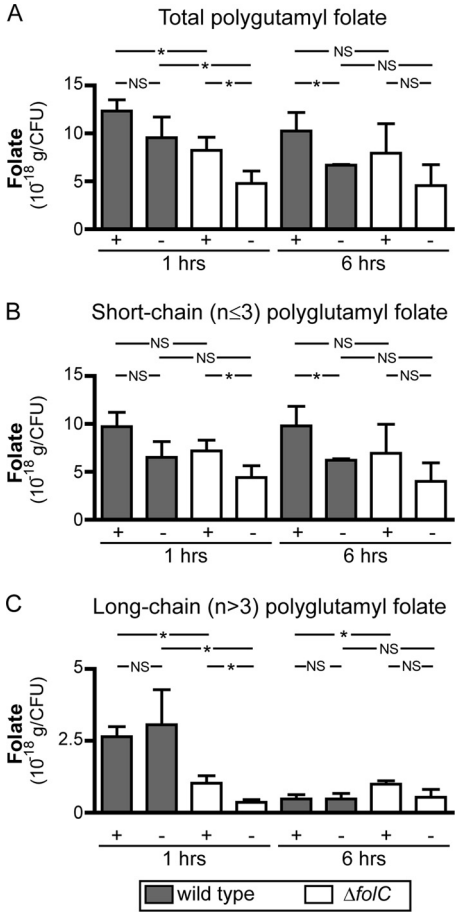

FIG 4 The level of intracellular long-chain polyglutamyl folate in *S. pneumoniae* depends on the presence of the *folC* gene. The R6 and LKIPB02 (Δ*folC*) strains were cultured in CO_2-rich (+) and CO_2-poor (−) BHI broth, and bacterial cells were collected at 1 and 6 h postinoculation. Intracellular folate levels were determined with a microbiological folate assay. (A and B) Total folate (A) and short-chain ($n \leq 3$) polyglutamyl folate (B) levels were determined in the presence and absence of human serum, respectively. (C) Levels of long-chain ($n > 3$) polyglutamyl folate were calculated by subtraction of the amount of short-chain polyglutamyl folate from the amount of total folate. Error bars represent standard deviations. Asterisks and "NS" mark significant and nonsignificant changes, respectively, in intracellular folate levels between the R6 and LKIPB02 strains that were grown under the same conditions.

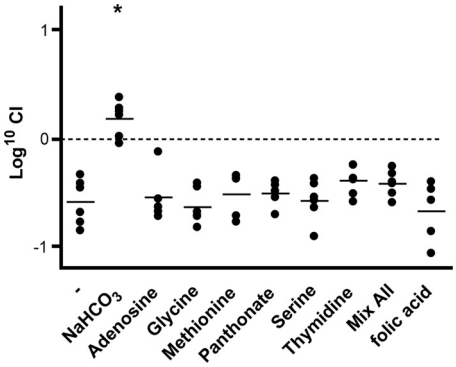

FIG 5 Metabolic complementation of the *S. pneumoniae* R6 Δ*folC* strain. The results of competitive growth of the LKIPB02 (Δ*folC*) strain with the R6 strain under CO_2-poor versus CO_2-rich conditions in BHI broth cultures without (−) or with $NaHCO_3$ (10 mM), folic acid (1 μg ml^{-1}), or the folate-dependent metabolites adenosine (20 μg ml^{-1}), glycine (50 μg ml^{-1}), methionine (50 μg ml^{-1}), pantothenate (1 μg ml^{-1}), serine (50 μg ml^{-1}), and/or thymidine (200 μg ml^{-1}) are shown. Symbols and horizontal lines mark individual and mean $\log_{10}$ CI scores, respectively, from cultures after approximately 6 h of growth. The asterisk marks the $\log_{10}$ CI score that was significantly different from that of the uncomplemented culture ($P < 0.05$).

metabolites did not significantly compensate for the LKIPB02 growth restriction under CO_2-poor conditions. Hence, the CO_2-dependent growth characteristics of the LKIPB02 strain could not be attributed to a specific folate-dependent metabolic pathway.

DISCUSSION

The respiratory tract pathogen *S. pneumoniae* needs to adapt to a wide variety of conditions it encounters during host colonization, infection, and transmission. Although environmental CO_2 levels inside and outside the human host can vary up to 100-fold, relatively little is known about the genetic factors that contribute to an adequate response of this bacterium to a change in CO_2 availability. By generating a large random *S. pneumoniae* R6 mutant library and exposing it to CO_2-poor and CO_2-rich culture conditions, we were able to demonstrate with the Tn-seq technology that the adaptation of *S. pneumoniae* to a CO_2-poor environment depends on carbonic anhydrase (PCA) activity and FolC-mediated long-chain polyglutamyl folate biosynthesis.

Carbonic anhydrases catalyze the reversible hydration of CO_2 to HCO_3^- and are important during the growth of bacterial, yeast, and fungal species under the relatively CO_2-poor conditions of ambient air (7). The impact of carbonic anhydrases on CO_2-dependent microbial growth is indirect, and nutritional supplementation of microbial cultures can often revert the observed growth defect of carbonic anhydrase mutant strains under CO_2-poor conditions (5, 6). We previously showed that PCA is required for *S. pneumoniae* growth under CO_2-poor conditions (8). Supplementation of an *S. pneumoniae* Δ*pca* strain with unsaturated fatty acids restored growth under CO_2-poor conditions, suggesting that PCA's enzymatic activity facilitates the HCO_3^--dependent conversion of acetyl-coenzyme A (CoA) to malenoyl-CoA. Besides fatty acid biosynthesis, several other *S. pneumoniae* enzymatic pathways depend on HCO_3^- as an essential substrate, e.g., arginine and uracil biosynthesis via carbamoyl-phosphate synthase (PurE and PurK) and aspartic acid and threonine biosynthesis via phosphoenolpyruvate carboxylase (Ppc). The presence of transposon mutations in the *purK* and *ppc* genes in our *S. pneumoniae* R6 mutant library suggests that these HCO_3^--dependent anabolic pathways are not essential under the nutrient-rich growth conditions used in this study. However, it is likely that the importance of PCA for the biosynthesis of various essential amino and nucleic acids will increase when *S. pneumoniae* is exposed to a nutrient-deprived CO_2-poor environment.

Bacterial FolC enzymes are often bifunctional (21). As a dihydrofolate synthase (DHFS), FolC catalyzes the ATP-dependent glutamylation of dihydropteroate to form DHF. DHF is a precursor of tetrahydrofolate (THF), which is essential for the biosynthesis of purines, pyrimidines, various amino acids (i.e., serine, glycine, and methionine), and pantothenate, as well as for the initiation of protein biosynthesis (i.e., $tRNA^{Met}$). In several bacterial species, FolC also functions as a folylpolyglutamate synthase (FPGS), which adds multiple glutamates onto THF to generate

polyglutamyl folate. The latter activity alters the specificity of THF as a cofactor or inhibitor of folate-dependent enzymes, and importantly, a long polyglutamyl chain prevents the cellular release of folate (22). Interestingly, both enzymatic functions of FolC do not require CO_2 or HCO_3^- as a substrate. However, the crystal structure of the *E. coli* FolC homolog has revealed a conserved carbamoylated lysine that is essential for FolC enzymatic activity (23, 24). This implies that FolC depends on CO_2 as an essential cofactor. Lysine carbamoylation occurs in various proteins, such as hemoglobin (25), urease (26), and class D β-lactamases (27), where it is implicated in the stabilization of a metal ligand or acts as an active-site residue. The formation of carbamoylated lysine is reversible and depends on environmental CO_2 levels (26), which explains our observation that folate biosynthesis and environmental CO_2 levels are intimately linked.

S. pneumoniae R6 encodes two FolC homologs, spr0178 (FolC) and spr0267 (SulB), which both have the conserved, putatively carbamoylated lysine. Interestingly, the *S. pneumoniae* R6 mutant library in this study only contained mutants with mutations in the spr0178 gene, while mutants with mutations in the spr0267 gene were not recovered. The *S. pneumoniae* spr0267 gene was previously shown to complement the methionine-dependent growth defect of an *E. coli* Δ*folC* strain (28). It shares an operon with three other folate biosynthetic genes, i.e., those coding for the dihydropteroate synthase SulA, the GTP cyclohydrolase SulC, and the bifunctional dihydropteroate synthase/hydroxymethyldihydropterin pyrophosphokinase SulD. Since other studies also failed to disrupt the *S. pneumoniae* spr0267 gene (13, 29), it is very likely that it is absolutely essential for pneumococcal growth. This suggests that the spr0267-encoded SulB enzyme has a central role in *S. pneumoniae* folate biosynthesis. The role of the second *S. pneumoniae* FolC homolog, encoded by the spr0178 gene in R6, is unknown. Despite the fact that many microorganisms express two FolC homologs (30), the molecular function of this second genomic copy of FolC has been poorly studied. Previously, we have shown in a genomic screen that the *S. pneumoniae* TIGR4 homolog of the spr0178 gene (SP_0197) is essential for bacterial replication during experimental meningitis (31), which suggests that this FolC homolog is required for niche adaptation. Metabolic engineering of the dairy bacterium *Lactococcus lactis* revealed that FolC overexpression can increase the cellular retention of folate as a result of folate polyglutamylation (32). Although we also observed increased folate polyglutamylation levels in the R6 wild-type strain compared to the folate polyglutamylation levels in the Δspr0178 strain, this phenomenon did not appear to depend on high levels of spr0178 expression. Hence, it is more plausible that the spr0267-encoded SulB enzyme is primarily involved in DHF biosynthesis, whereas the spr0178-encoded FolC enzyme is primarily required to meet the conditional and growth-phase-dependent demand for folate polyglutamylation.

Folic acid supplementation did not rescue the growth restriction of the *S. pneumoniae* Δ*folC* strain under CO_2-poor conditions. Most likely, this is best explained by the fact that *S. pneumoniae* does not encode a folate transporter homolog to make use of the supplemented folic acid (33, 34). However, even if uptake of folic acid still occurred, the FPGS activity of FolC would be required to convert it to long-chain ($n > 3$) polyglutamyl folate, which is the preferred cofactor for various essential metabolic functions (22). We were also unable to link the growth defect of the *S. pneumoniae* Δ*folC* strain to a particular metabolic pathway. This can be explained by the fact that folate is involved not only in nucleic, amino, and pantothenic acid biosynthesis (21) but also in the biosynthesis of formylated methyonyl-tRNA ($tRNA^{Met}$) (35, 36). This compound is essential for the initiation of protein biosynthesis, and a shortage of cellular formylated $tRNA^{Met}$ will reduce microbial growth rates (37). As this cellular compound cannot be taken up from the environment, it needs to be synthesized *de novo*.

Despite the fact that CO_2 or HCO_3^- appears to have an essential role in the biosynthesis of membrane fatty acids and the important cellular cofactor polyglutamyl folate, only 2 of the 1,538 genes that were assayed for essentiality during *S. pneumoniae* growth under CO_2-poor conditions passed our Tn-seq selection criteria. In an attempt to select more target genes, we tried to set our selection criteria at a less-stringent level. However, this consistently resulted in the identification of more false positives besides spr1317 (data not shown). It is also very unlikely that the mutant library used in this study was too small to cover all potential mutants important for *S. pneumoniae* adaptation to CO_2-poor conditions. In earlier studies, it was possible to target between 1,322 (9) and 1,689 (13) *S. pneumoniae* genes, which relates very well to the total of 1,538 genes for which mutants were found in this study. Furthermore, rarefaction analysis (11) confirmed that our *S. pneumoniae* library had reached saturation for the number of genes that could potentially be hit by a transposon. It is therefore likely that the lack of targets in this study is the direct consequence of our assay conditions. An experimental explanation for the lack of targets in this Tn-seq experiment could be the fact that growth defects in mutants could be cross-complemented by diffusible products provided by other mutants in the library. In this study, the diffusion of endogenous CO_2 or metabolites released by other mutants in the library could potentially have interfered with the readout of our experiments. This would, for example, explain the large difference in the growth defect of the *pca* mutant strain in the library screen, i.e., 15-fold, and in the competition validation experiments, i.e., >1,000-fold. However, this phenomenon was not observed for the Δ*folC* strain, since here the Tn-seq and the competition validation results were very comparable. Therefore, the differences in the results for the Δ*pca* strain in the Tn-seq and validation experiments were most likely caused by differences in the readout method. In the Tn-seq experiment, readout was based on the amount of genomic DNA extracted from both viable and nonviable bacteria after the challenge, whereas in the validation experiments, the outcome was based on viable bacterial counts. Since the Δ*pca* strain presented fast autolysis after a period of growth under CO_2-poor conditions, the amount of chromosomal DNA from nonviable cells that contributed to the Tn-seq signal could have been considerable.

In retrospect, the number of genes that could be potentially be identified by this Tn-seq screen is rather limited. There are only three types of responses that can compensate for the lack of environmental CO_2: (i) increased production and/or retention of endogenous CO_2/HCO_3^-, (ii) the expression of metabolic pathways that compensate for the low availability of CO_2/HCO_3^- as a substrate, and (iii) the expression of genes that compensate for the low availability of CO_2/HCO_3^- as a cofactor. PCA clearly belongs to the first class of genes, because the reversible hydration of CO_2 to HCO_3^- prevents the passive diffusion of endogenous CO_2 from cells. Interestingly, we did not identify genes that contribute to endogenous CO_2 production, such as the oxygen-dependent

pyruvate oxidase (SpxB) that is responsible for the generation of endogenous CO_2 from pyruvate. It is possible that *S. pneumoniae* switches from aerobiosis to anaerobiosis before cellular CO_2/HCO_3^- stocks have been depleted. In anaerobiosis, most *S. pneumoniae* fermentative pathways yield acetic and lactic acid instead of CO_2 (19), implying that endogenous CO_2 production results from various minor metabolic pathways (7). No genes from the second class, which compensate for the low availability of environmental CO_2/HCO_3^- as a substrate, were identified in our study. This can be explained by the fact that, except for the Δ*pca* strain itself, all mutants express PCA. In the presence of PCA, cellular depletion of HCO_3^- will not occur, which means that HCO_3^--dependent metabolic pathways will not be hampered by environmental CO_2-poor conditions. FolC should be ranked to the third class of genes, which compensate for a low availability of environmental CO_2 as a cofactor. Although FolC is still expected to use CO_2 as a cofactor, the expression of two FolC copies (i.e., SulB and FolC) must compensate for the conditional decrease in intracellular long-chain polyglutamyl folate. The Tn-seq screen did not identify other genes of the third class, but the identification of FolC implies that all proteins with a carbamoylated lysine could potentially respond to changes in environmental CO_2. For instance, the cell wall precursor muramoyl ligases MurD, MurE, and MurF, which are distantly related to FolC, and alanine racemace all have a carbamoylated lysine that is essential for enzymatic activity (38, 39). This implies that alteration of environmental CO_2 levels could potentially affect more cellular pathways than we have previously anticipated.

In conclusion, we demonstrated by using the Tn-seq technology that the adaptive response of *S. pneumoniae* to CO_2-poor conditions entails PCA-mediated retention of endogenous CO_2 to feed fatty acid biosynthesis and FolC-dependent polyglutamyl folate biosynthesis. These results have given us new insight into the role of CO_2 in critical cellular processes of this respiratory tract pathogen, which will further improve our understanding of *S. pneumoniae* niche adaptation.

ACKNOWLEDGMENTS

This work was financially supported by Horizon Breakthrough grant 93518023 (P.B.) and Horizon Valorization grant 93515506 (P.B.) from the Netherlands Genomics Initiative and by the European Commission through FP7 Marie Curie IEF Action 274586 (A.L.Z.).

REFERENCES

1. **Bogaert D, de Groot R, Hermans PW.** 2004. *Streptococcus pneumoniae* colonisation: the key to pneumococcal disease. Lancet Infect. Dis. **4**:144–154.
2. **Kadioglu A, Weiser JN, Paton JC, Andrew PW.** 2008. The role of *Streptococcus pneumoniae* virulence factors in host respiratory colonization and disease. Nat. Rev. Microbiol. **6**:288–301.
3. **Austrian R, Collins P.** 1966. Importance of carbon dioxide in the isolation of pneumococci. J. Bacteriol. **92**:1281–1284.
4. **Kempner W, Schlayer C.** 1942. Effect of CO_2 on the growth rate of the Pneumococcus. J. Bacteriol. **43**:387–396.
5. **Aguilera J, Van Dijken JP, De Winde JH, Pronk JT.** 2005. Carbonic anhydrase (Nce103p): an essential biosynthetic enzyme for growth of *Saccharomyces cerevisiae* at atmospheric carbon dioxide pressure. Biochem. J. **391**:311–316.
6. **Bahn YS, Cox GM, Perfect JR, Heitman J.** 2005. Carbonic anhydrase and CO_2 sensing during *Cryptococcus neoformans* growth, differentiation, and virulence. Curr. Biol. **15**:2013–2020.
7. **Smith KS, Ferry JG.** 2000. Prokaryotic carbonic anhydrases. FEMS Microbiol. Rev. **24**:335–366.
8. **Burghout P, Cron LE, Gradstedt H, Quintero B, Simonetti E, Bijlsma JJ, Bootsma HJ, Hermans PW.** 2010. Carbonic anhydrase is essential for *Streptococcus pneumoniae* growth in environmental ambient air. J. Bacteriol. **192**:4054–4062.
9. **Bijlsma JJ, Burghout P, Kloosterman TG, Bootsma HJ, de Jong A, Hermans PW, Kuipers OP.** 2007. Development of genomic array footprinting for identification of conditionally essential genes in *Streptococcus pneumoniae.* Appl. Environ. Microbiol. **73**:1514–1524.
10. **Hensel M.** 1998. Whole genome scan for habitat-specific genes by signature-tagged mutagenesis. Electrophoresis **19**:608–612.
11. **Goodman AL, McNulty NP, Zhao Y, Leip D, Mitra RD, Lozupone CA, Knight R, Gordon JI.** 2009. Identifying genetic determinants needed to establish a human gut symbiont in its habitat. Cell Host Microbe **6**:279–289.
12. **Langridge GC, Phan MD, Turner DJ, Perkins TT, Parts L, Haase J, Charles I, Maskell DJ, Peters SE, Dougan G, Wain J, Parkhill J, Turner AK.** 2009. Simultaneous assay of every *Salmonella* Typhi gene using one million transposon mutants. Genome Res. **19**:2308–2316.
13. **van Opijnen T, Bodi KL, Camilli A.** 2009. Tn-seq: high-throughput parallel sequencing for fitness and genetic interaction studies in microorganisms. Nat. Methods **6**:767–772.
14. **Burghout P, Bootsma HJ, Kloosterman TG, Bijlsma JJ, de Jongh CE, Kuipers OP, Hermans PW.** 2007. Search for genes essential for pneumococcal transformation: the RadA DNA repair protein plays a role in genomic recombination of donor DNA. J. Bacteriol. **189**:6540–6550.
15. **Samsbrook J, Fritsch EF, Maniatis T.** 1989. Molecular cloning: a laboratory manual. Cold Spring Harbor Laboratory Press, Cold Spring Harbor, NY.
16. **Zomer A, Burghout P, Bootsma HJ, Hermans PW, van Hijum SA.** 2012. ESSENTIALS: Software for rapid analysis of high throughput transposon insertion sequencing data. PLoS One **7**:e43012. doi:10.1371/journal.pone.0043012.
17. **Guiral S, Henard V, Laaberki MH, Granadel C, Prudhomme M, Martin B, Claverys JP.** 2006. Construction and evaluation of a chromosomal expression platform (CEP) for ectopic, maltose-driven gene expression in *Streptococcus pneumoniae.* Microbiology **152**:343–349.
18. **Horne DW, Patterson D.** 1988. *Lactobacillus casei* microbiological assay of folic acid derivatives in 96-well microtiter plates. Clin. Chem. **34**:2357–2359.
19. **Hoskins J, Alborn WE, Jr, Arnold J, Blaszczak LC, Burgett S, DeHoff B, Estrem ST, Fritz L, Fu DJ, Fuller W, Geringer C, Gilmour R, Glass JS, Khoja H, Kraft AR, Lagace RE, LeBlanc DJ, Lee LN, Lefkowitz EJ, Lu J, Matsushima P, McAhren SM, McHenney M, McLeaster K, Mundy CW, Nicas TI, Norris FH, O'Gara M, Peery RB, Robertson GT, Rockey P, Sun PM, Winkler ME, Yang Y, Young-Bellido M, Zhao G, Zook CA, Baltz RH, Jaskunas SR, Rosteck PR, Jr, Skatrud PL, Glass JI.** 2001. Genome of the bacterium *Streptococcus pneumoniae* strain R6. J. Bacteriol. **183**:5709–5717.
20. **Tamura T, Shin YS, Williams MA, Stokstad EL.** 1972. *Lactobacillus casei* response to pteroylpolyglutamates. Anal. Biochem. **49**:517–521.
21. **Bognar AL, Osborne C, Shane B, Singer SC, Ferone R.** 1985. Folylpolygamma-glutamate synthase-dihydrofolate synthase. Cloning and high expression of the *Escherichia coli folC* gene and purification and properties of the gene product. J. Biol. Chem. **260**:5625–5630.
22. **McGuire JJ, Bertino JR.** 1981. Enzymatic synthesis and function of folylpolyglutamates. Mol. Cell. Biochem. **38 Spec No**:19–48.
23. **Mathieu M, Debousker G, Vincent S, Viviani F, Bamas-Jacques N, Mikol V.** 2005. *Escherichia coli* FolC structure reveals an unexpected dihydrofolate binding site providing an attractive target for anti-microbial therapy. J. Biol. Chem. **280**:18916–18922.
24. **Sun X, Cross JA, Bognar AL, Baker EN, Smith CA.** 2001. Folate-binding triggers the activation of folylpolyglutamate synthase. J. Mol. Biol. **310**:1067–1078.
25. **Arnone A.** 1974. X-ray studies of the interaction of CO_2 with human deoxyhaemoglobin. Nature **247**:143–145.
26. **Jabri E, Carr MB, Hausinger RP, Karplus PA.** 1995. The crystal structure of urease from *Klebsiella aerogenes.* Science **268**:998–1004.
27. **Golemi D, Maveyraud L, Vakulenko S, Samama JP, Mobashery S.** 2001. Critical involvement of a carbamylated lysine in catalytic function of class D beta-lactamases. Proc. Natl. Acad. Sci. U. S. A. **98**:14280–14285.
28. **Lacks SA, Greenberg B, Lopez P.** 1995. A cluster of four genes encoding enzymes for five steps in the folate biosynthetic pathway of *Streptococcus pneumoniae.* J. Bacteriol. **177**:66–74.
29. **Song JH, Ko KS, Lee JY, Baek JY, Oh WS, Yoon HS, Jeong JY, Chun J.** 2005. Identification of essential genes in *Streptococcus pneumoniae* by allelic replacement mutagenesis. Mol. Cells **19**:365–374.

30. **de Crecy-Lagard V, El Yacoubi B, de la Garza RD, Noiriel A, Hanson AD.** 2007. Comparative genomics of bacterial and plant folate synthesis and salvage: predictions and validations. BMC Genomics **8**:245.
31. **Molzen TE, Burghout P, Bootsma HJ, Brandt CT, van der Gaast-de Jongh CE, Eleveld MJ, Verbeek MM, Frimodt-Moller N, Ostergaard C, Hermans PW.** 2011. Genome-wide identification of *Streptococcus pneumoniae* genes essential for bacterial replication during experimental meningitis. Infect. Immun. **79**:288–297.
32. **Sybesma W, Starrenburg M, Kleerebezem M, Mierau I, de Vos WM, Hugenholtz J.** 2003. Increased production of folate by metabolic engineering of *Lactococcus lactis.* Appl. Environ. Microbiol. **69**:3069–3076.
33. **Henderson GB, Zevely EM, Kadner RJ, Huennekens FM.** 1977. The folate and thiamine transport proteins of *Lactobacillus casei.* J. Supramol. Struct. **6**:239–247.
34. **Kumar HP, Tsuji JM, Henderson GB.** 1987. Folate transport in *Lactobacillus salivarius.* Characterization of the transport mechanism and purification and properties of the binding component. J. Biol. Chem. **262**: 7171–7179.
35. **Clark FC, Marcker KA.** 1965. Coding response of N-fromyl-methionyl-sRNA to UUG. Nature **207**:1038–1039.
36. **Dickerman HW, Steers E, Jr, Redfield BG, Weissbach H.** 1967. Methionyl soluble ribonucleic acid transformylase. I. Purification and partial characterization. J. Biol. Chem. **242**:1522–1525.
37. **Harvey RJ.** 1973. Growth and initiation of protein synthesis in *Escherichia coli* in the presence of trimethoprim. J. Bacteriol. **114**:309–322.
38. **Dementin S, Bouhss A, Auger G, Parquet C, Mengin-Lecreulx D, Dideberg O, van Heijenoort J, Blanot D.** 2001. Evidence of a functional requirement for a carbamoylated lysine residue in MurD, MurE and MurF synthases as established by chemical rescue experiments. Eur. J. Biochem. **268**:5800–5807.
39. **Im H, Sharpe ML, Strych U, Davlieva M, Krause KL.** 2011. The crystal structure of alanine racemase from *Streptococcus pneumoniae*, a target for structure-based drug design. BMC Microbiol. **11**:116. doi:10.1186/1471-2180-11-116.
40. **Hanahan D.** 1983. Studies on transformation of *Escherichia coli* with plasmids. J. Mol. Biol. **166**:557–580.
41. **Martin B, Prudhomme M, Alloing G, Granadel C, Claverys JP.** 2000. Cross-regulation of competence pheromone production and export in the early control of transformation in *Streptococcus pneumoniae.* Mol. Microbiol. **38**:867–878.